

Microstructural characteristics of SrTiO₃ nanoparticles: the role of capping ligand concentration

Uzma K.H. Bangi¹ ✉, Vipul M. Prakshale¹, WooJe Han³, Hyung-Ho Park³, Noor Mahmad N. Maldar², Lalasaheb P. Deshmukh¹

¹School of Physical Sciences, Solapur University, Kegaon, Solapur-413 255, M.S., India

²Polymer Chemistry Division, Solapur University, Kegaon, Solapur-413 255, M.S., India

³Department of Materials Science and Engineering, Yonsei University, Seoul 120-749, Republic of Korea

✉ E-mail: uzma.phys@gmail.com

Published in Micro & Nano Letters; Received on 3rd December 2015; Revised on 9th March 2016; Accepted on 9th March 2016

The role of capping ligand concentration on the microstructural characteristics of strontium titanate (SrTiO₃ or STO) nanoparticles has been investigated. Capping the surface of primary particles with ligand having long alkyl chain protects the increase in nanoparticle size by hindering the agglomeration. Therefore, in the present work the role of ligands namely cetyltrimethyl ammonium bromide (CTAB) and polyvinylpyrrolidone (PVP) on the structure and surface morphology of STO have been studied by varying their concentrations from 0.01 to 0.08 M and 0.001 to 0.008 M respectively. The structure of STO was determined using the X-ray diffraction (XRD) and transmission electron microscopy (TEM) techniques. The surface morphologies of the different STO samples were viewed through the field emission scanning electron microscopy (FESEM). A cubic crystalline phase formation of STO has been observed as revealed from the XRD and TEM images. The typical crystallite size, strain and dislocation density determined for PVP capped STO are 29 nm, 2.08×10^{-3} and $1.194 \times 10^{15} \text{ m}^{-2}$, respectively. FESEM images manifested a decrease in the grain size as a result of increase in the concentration of CTAB to 0.05 M and PVP to 0.005 M. Nearly spherical grains with some sort of fusing have been observed at lower and higher concentrations of the CTAB and PVP in both the cases.

1. Introduction: Nanoparticles of perovskite family are of enormous interest because of their utilisation in electronic, optical and sensing devices. Strontium titanate (SrTiO₃ or STO), an *n*-type semiconductor is one of these promising materials having cubic crystal system with variety of properties such as high dielectric constant (300), wide band-gap (3.2 eV), better corrosion resistance and higher flat band potential etc. Owing to these outstanding properties, STO can be employed in oxygen sensor, photocatalysis, organic thin film transistor and dye sensitised solar cells (DSSCs) etc. [1–4]. Amongst all these applications, DSSCs are widely studied due to their high efficiency, low cost and eco-friendly production. A DSSC typically composed of an anode, a sensitiser, a counter electrode and an electrolyte injected between sensitiser and counter electrode. Among them, anode is one of the key components consisting of wide band-gap nanoparticles governing the performance of DSSC. The mechanisms of DSSC such as dye adsorption [5], photoelectron injection [6], light scattering [7] and electron transport recombination [8] are directly influenced by the type of materials used for the anode. Generally, binary metal oxides like TiO₂ or ZnO nanoparticles were used as anodes in DSSCs [9, 10]. Moreover, studies on the surface modification of TiO₂ with an insulating layer of Al₂O₃ [11], SrTiO₃ [12] etc. have been carried out for increasing the efficiency of DSSC. However recently, ternary oxide semiconductor, such as STO nanoparticles is being used as photoanode in DSSC instead of TiO₂ nanoparticles [4, 13]. To date, the use of STO nanoparticles as photoanode in DSSC has been rarely reported. For the ease of preparation, low temperature wet-chemical techniques such as sol-gel, hydrothermal, solvothermal and precipitation are being used for the synthesis of STO nanoparticles [14–16]. Till now the studies on the synthesis of STO nanoparticles using different precursors [17] and doping [18] have been carried out employing

these techniques. However, the influence of different capping ligands concentration on the microstructural characteristics of STO nanoparticles was not much studied. It was observed that capping the surface of primary particles with a ligand reduces the size of nanoparticles [19]. Capping ligand prevents the agglomeration of growing particles by strongly binding their surface forming a stabilising capping layer around them. The growth of primary particles is affected by the steric effect of ligand skeleton. A study on the steric effects of ligand chain length and chain branching on nanoparticles size is reported elsewhere [20]. Therefore, the influence of cetyltrimethyl ammonium bromide (CTAB) and polyvinylpyrrolidone (PVP) concentrations on the structure and surface morphology of precipitated STO nanoparticles has been studied. CTAB and PVP are cationic and non-ionic ligands having different structural effects due to their chain length on the synthesis of nanoparticles. The chemistry of CTAB and PVP in particular their chain length (molecular weight) plays a key role in controlling the materials characteristics. Therefore, in this Letter special attention was given to the concentrations of CTAB and PVP as they also control structure and morphology of STO. The as synthesised STO nanoparticles can be employed in DSSC as photoanode.

2. Experimental: The synthesis of STO nanoparticles was carried out using the AR purity chemicals purchased from sigma Aldrich. Strontium nitrate [Sr(NO₃)₂, 99.9%] and potassium titanyl oxalate [PTOX or K₂TiO(C₂O₄)₂, 99%] were used as starting materials while CTAB (364.45 g) and PVP (mol. wt. 40,000 g) as capping ligands. Deionised (DI) water and ethanol (EtOH) were used for precipitate formation and washing purpose. The experimental procedure for the synthesis of STO nanoparticles is presented in Fig. 1.

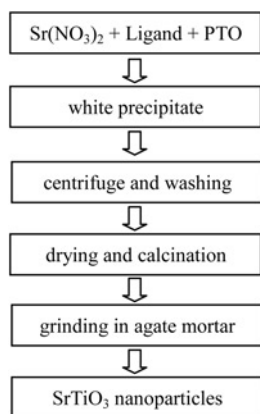
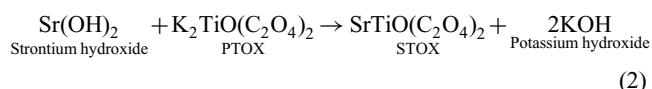
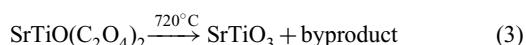


Fig. 1 Experimental flowchart for the synthesis of STO nanoparticles

Initially, the aqueous solutions of $\text{Sr}(\text{NO}_3)_2$ and capping ligand (CTAB or PVP) were mixed and stirred for 30 min. Later, PTOX was added dropwise to this solution forming the white precipitate (STOX) which was again stirred for 30 min. The formation of STO precipitate may occur via following chemical reactions (1) and (2)



$\text{Sr}(\text{NO}_3)_2$ on dilution may form $\text{Sr}(\text{OH})_2$ as seen from (1). The addition of CTAB or PVP caps the surface of $\text{Sr}(\text{OH})_2$ via N and O atoms [19]. Afterwards, the dropwise addition of PTOX in this solution may form the STOX along with the byproduct KOH (2). KOH can be removed from the precipitate by repeated washing with D.I. water. The as formed precipitate was centrifuged at 10,000 rpm for 10 min and washed thrice with DI water and then EtOH to again remove impurity. The washed precipitate was dried at 40°C for 24 h and decomposed to STO after calcination at 720°C for 1 h at a heating rate of 5°C/min [21] (3).



The product was cooled to R.T. and grinded in agate mortar for the characterisation purpose. The effects of varying concentrations of CTAB (0.01–0.08 M) and PVP (0.001–0.008 M) on the microstructural characteristics of STO were studied.

To confirm the crystalline structure of STO, XRD (using Ultima model, Rigaku, Japan) was performed and analysed with $\text{Cu K}\alpha$ radiation of wavelength 1.541 Å at 2θ values ranging from 20° to 80°. The morphological images of the STO samples were obtained using field emission scanning electron microscopy (FESEM, JSM-600F, JEOL, Japan). Moreover, transmission electron microscopy (TEM, JEM- 2100F, JEOL, Japan) was utilised to characterise the size and shape of the STO particles.

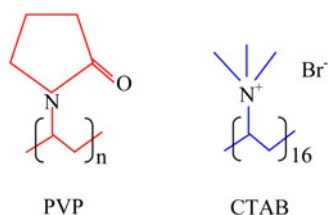


Fig. 2 Molecular structures of PVP and CTAB

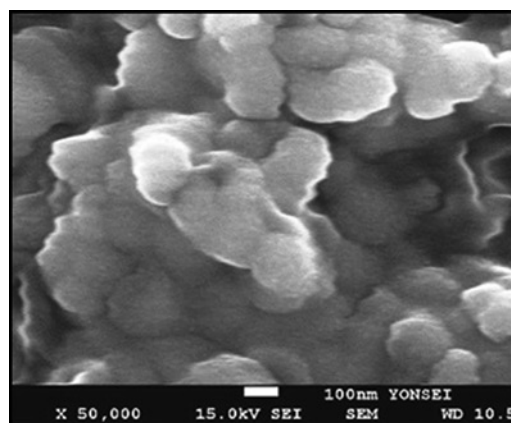


Fig. 3 FESEM image of pristine STO sample

3. Results and discussion: The capping ligand controls the size of nanoparticles by forming a protective layer around the particles' surface during the growth process. Ligand consists of a head group which anchors the surface of particle and a tail group (alkyl chain) which is away from the surface floating in the dilute medium. The broad area of head and the long alkyl chain of tail of the ligand sterically affect the size of nanoparticles. CTAB and PVP were used as capping ligand for the synthesis of STO nanoparticles. CTAB is a cationic ligand with cetyl chain connected to N and Br ions (Fig. 2) while PVP is a non-ionic ligand with a polyalkyl chain connected to pentane ring containing N and O donor atoms (Fig. 2).

Because of the small chain length of CTAB (cetyl) as compared with PVP (polyalkyl), the concentration of CTAB chosen for the synthesis was higher than PVP (CTAB:PVP::10:1). Therefore, the influence of varying concentrations of CTAB (typically 0.01, 0.05, and 0.08 M) and PVP (typically 0.001, 0.005, and 0.008 M) on the structure and surface morphology of STO particles was studied. STO samples were prepared by keeping the concentrations

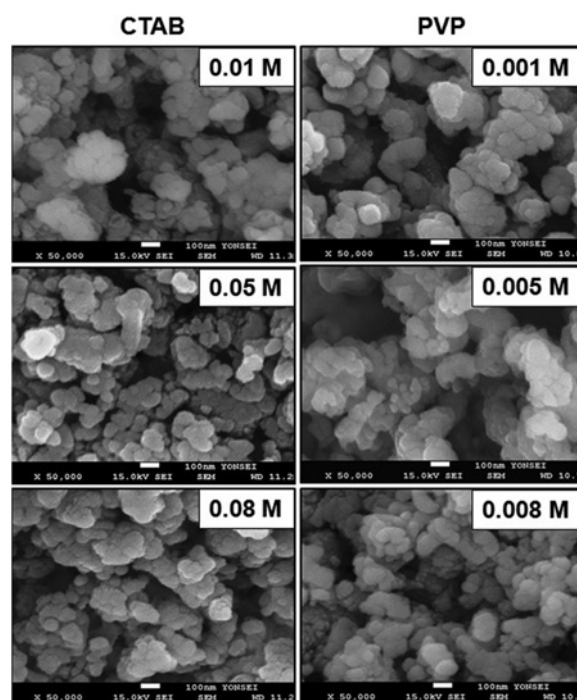


Fig. 4 FESEM images of STO samples for varying concentration of CTAB and PVP

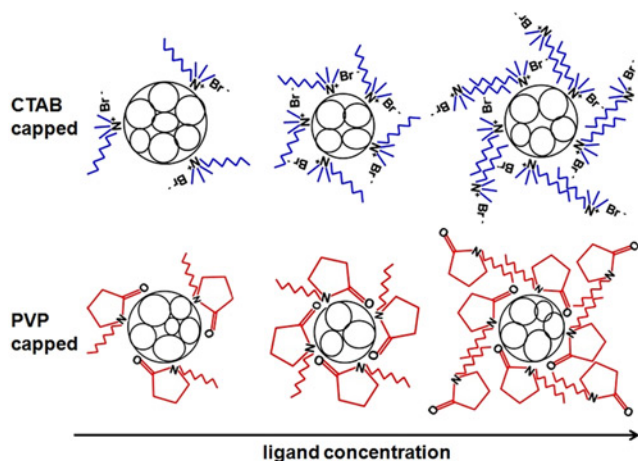


Fig. 5 Pictorial representation of varying concentrations CTAB and PVP capping to the particles' surface

of $\text{Sr}(\text{NO}_3)_2$ and PTOX fixed to 0.05 M and volume ratio of $\text{Sr}(\text{NO}_3)_2$:PTOX:Ligand to 1:1:0.05.

Fig. 3 is the FESEM image of pristine STO sample which exhibit the coalescence of particles with larger size and non-uniform shapes.

The FESEM images of STO samples synthesised using various concentrations of CTAB (0.01, 0.05, 0.08 M) and PVP (0.001, 0.005, 0.008 M) are shown in Fig. 4. It is seen that the grain size of the STO reduced with increase in CTAB concentration from 0.01 to 0.05 M and PVP concentration from 0.001 to 0.005 M (Fig. 4). The larger grain size of STO at low concentration of ligand may be due to the incomplete capping of ligand to the surface of primary particles. More primary particles may permeate through the capping layer so as to deposit new atoms to the surface resulting in agglomerated particles [20]. Moreover, at high concentration of CTAB (>0.05 M) and PVP (>0.005 M) the particles seem to be highly aggregated. This may be due the presence of more ligand molecules forming a double layer (with inverted polarity) around the surface of particle which attracts another particle causing agglomeration grains [19]. STO samples synthesised using 0.05 M of CTAB and 0.005 M of PVP exhibit comparatively smaller grains than other STO samples. Thus, these concentrations of CTAB and PVP are sufficient to form a stabilising capping layer around the surface of particles preventing their agglomeration [20]. However, among the CTAB (0.05 M) and PVP (0.005 M) capped

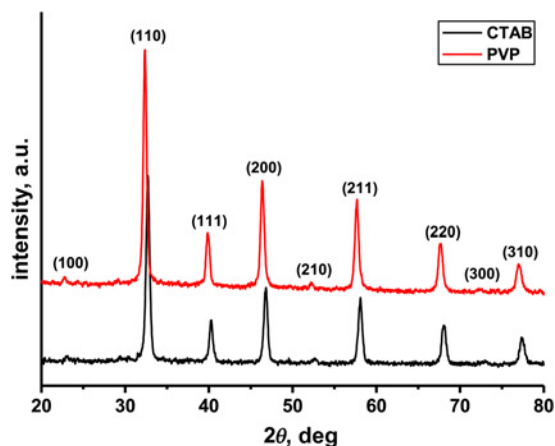


Fig. 6 Diffractogram of typical STO samples prepared using ligands CTAB and PVP

Table 1 Average crystallite size, strain and dislocation density of STO samples synthesised using CTAB (0.05 M) and PVP (0.005 M)

Samples	CTAB capped	PVP capped
average crystallite size (D) nm	28.19	29.01
strain (ϵ)	2.24×10^{-3}	2.08×10^{-3}
dislocation density (δ) m^{-2}	1.25×10^{15}	1.19×10^{15}

STO samples, the later one shows less agglomerated grains arranged in network structure.

The influence of varying concentrations of CTAB and PVP on the morphology of STO samples can also be understood by the pictorial representation as shown in Fig. 5. From Fig. 5 it is clear that PVP occupy much area of the surface of STO due to its larger head group while CTAB partially coordinates the particle surface. This clears that the higher concentration of CTAB is needed to completely cap the surface of STO particles.

XRD diffractogram of the typical STO samples prepared using ligands CTAB (0.05 M) and PVP (0.005 M) are shown in Fig. 6. From Fig. 6 it is obvious that STO has cubic crystal structure matching with the JCPDS data card number PDF#350734. Both the diffractograms exhibit a sharper and stronger peak of (110) indicating phase orientation along $\langle 110 \rangle$. The absence of impurity peak (KOH) manifest that the calcinations temperature of 720°C is sufficient for the formation of cubic STO from STOX and for the evolution of impurities.

Table 1 shows the average crystallite size, strain induced and dislocation density of the STO samples prepared using CTAB and PVP. From Table 1 it is clear that the average crystallite size determined for CTAB capped STO sample is 28 nm which is not much smaller than PVP capped STO (29 nm). However, this result is contradictory to the FESEM images (Fig. 4) because the PVP capped STO has less agglomerated grains than CTAB capped STO sample. Therefore, the TEM has been performed for the PVP (0.005 M) capped STO sample.

Fig. 7 shows the TEM images of PVP capped STO sample at two different magnifications (a) 20 nm and (b) 5 nm. The dark black spots are the STO nanoparticles with the grey layer around their surface which is of PVP [19]. Though it shows the

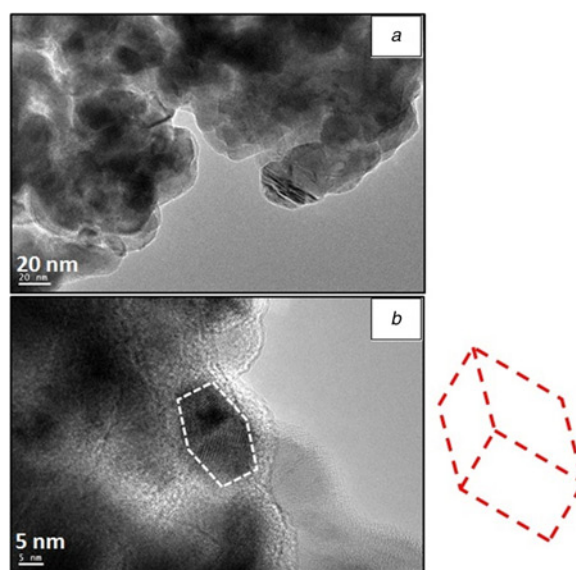


Fig. 7 TEM images of PVP (0.005 M) capped STO sample (different magnification)
a 20 nm
b 5 nm

hexagonal geometry (white dashed line) of the STO crystal, but it is actually nanocuboid of STO (shown at R.H.S) [22] with the particles size of 30 nm. These results are in good agreement with the XRD data.

4. Conclusions: The influence of varying concentrations of CTAB and PVP on the microstructural characteristics of STO was studied in detail. STO nanoparticles can be synthesised using cost-effective method of precipitation. STO nanoparticles with cubic crystal structure and average crystallite size of 29 nm were synthesised as confirmed from the XRD and TEM observations. It is found that the particle size of STO decreased with increase in the CTAB and PVP concentrations which further increased with their concentration as revealed from FESEM images. The as synthesised STO nanoparticles can be employed as a photoanode in DSSC.

5. Acknowledgments: This study was financially supported by the Department of Science and Technology – Science & Engineering Research Board (DST-SERB), New Delhi, India, through a major research project on ‘aerogels’ (no. SB/FTP/PS-030/2014). One of the authors, Uzma K. H. Bangi, is very grateful to the DST-SERB for Young Scientist Fellowship under fast-track scheme.

6 References

- [1] Voigts F., Damjanovi T., Borchardt G., *ET AL.*: ‘Synthesis and characterization of strontium titanate nanoparticles as potential high temperature oxygen sensor material’, *J. Nanomat.*, 2006, **2006**, pp. 1–6
- [2] Sulaeman U., Yin S., Sato T.: ‘Solvothermal synthesis of designed nonstoichiometric strontium titanate for efficient visible-light photocatalysis’, *Appl. Phys. Lett.*, 2010, **97**, pp. 103102–103104
- [3] Cai Q.J., Gan Y., Chan-Park M.B., *ET AL.*: ‘Solution-processable barium titanate and strontium titanate nanoparticle dielectrics for low-voltage organic thin-film transistors’, *Chem. Mater.*, 2009, **21**, pp. 3153–3161
- [4] Chen C., Dai Q., Miao C., *ET AL.*: ‘Strontium titanate nanoparticles as the photoanode for CdS quantum dot sensitized solar cells’, *RSC Adv.*, 2015, **5**, pp. 4844–4852
- [5] Sauvage F., Decoppet J.D., Zhang M., *ET AL.*: ‘Effect of sensitizer adsorption temperature on the performance of dye-sensitized solar cells’, *J. Am. Chem. Soc.*, 2011, **133**, pp. 9304–9310
- [6] Tiwana P., Docampo P., Johnston M.B., *ET AL.*: ‘. Electron mobility and injection dynamics in mesoporous ZnO, SnO₂, and TiO₂ films used in dye-sensitized solar cells’, *ACS Nano*, 2011, **5**, pp. 5158–5166
- [7] Huang F., Chen D., Zhang X.L., *ET AL.*: ‘Dual-function scattering layer of submicrometer-sized mesoporous TiO₂ beads for high-efficiency dye-sensitized solar cells’, *Adv. Funct. Mater.*, 2010, **20**, pp. 1301–1305
- [8] Liao J.Y., Lei B.X., Kuang D.B., *ET AL.*: ‘Tri-functional hierarchical TiO₂ spheres consisting of anatase nanorods and nanoparticles for high efficiency dye-sensitized solar cells’, *Energy Environ. Sci.*, 2011, **4**, pp. 4079–4085
- [9] Shin K., Jun Y., Han G.Y., *ET AL.*: ‘Effect of incorporation of TiO₂ nanoparticles into oriented TiO₂ nanotube based dye-sensitized solar cells’, *J. Nanosci. Nanotechnol.*, 2009, **9**, (12), pp. 7436–7439
- [10] Lee T.-H., Sue H.-J., Cheng X.: ‘Solid-state dye-sensitized solar cells based on ZnO nanoparticle and nanorod array hybrid photoanodes’, *Nanoscale Res. Lett.*, 2011, **6**, (1), pp. 517–524
- [11] Gao X., Guan D., Huo J., *ET AL.*: ‘Free standing TiO₂ nanotube array electrodes with an ultra-thin Al₂O₃ barrier layer and TiCl₄ surface modification for highly efficient dye sensitized solar cells’, *Nanoscale*, 2013, **5**, pp. 10438–10446
- [12] Kim C.W., Suh S.P., Choi M.J., *ET AL.*: ‘Fabrication of SrTiO₃–TiO₂ heterojunction photoanode with enlarged pore diameter for dye-sensitized solar cells’, *J. Mater. Chem. A*, 2013, **1**, pp. 11820–11827
- [13] Gholamrezaei S., Salavati-Niasari M.: ‘Natural sensitizer for low cost dye sensitized solar cell based on strontium titanate nanoparticles’, *J. Mater. Sci. Mater. Electron*, 2016, **27**, (3), pp. 2467–2472
- [14] Fuentes S., Zarate R.A., Chavez E., *ET AL.*: ‘Preparation of SrTiO₃ nanomaterial by a sol–gel-hydrothermal method’, *J. Mater. Sci.*, 2010, **45**, (6), pp. 1448–1452
- [15] Márquez-Herrera A., Ovando-Medina V.M., Corona-Rivera M.A., *ET AL.*: ‘A novel solvothermal route for obtaining strontium titanate nanoparticles’, *J. Nanopart. Res.*, 2013, **15**, pp. 1525–1531
- [16] Yan W.B., Gao F., Hua J., *ET AL.*: ‘Preparation of nanosized strontium titanate powder by a nitrilotriacetate precipitation method’, *Adv. Mater. Res.*, 2013, **734**, pp. 2324–2327
- [17] Li Y.Y., Hao H.S., Qin L., *ET AL.*: ‘Synthesis and characterization of Ho³⁺ doped strontium titanate down conversion nanocrystals and its application in dye-sensitized solar cells’, *J. Alloys Comp.*, 2015, **622**, pp. 1–7
- [18] Chen D., Jiao X., Zhang M.: ‘Hydrothermal synthesis of strontium titanate powders with nanometer size derived from different precursors’, *J. Euro. Ceram. Soc.*, 2000, **20**, pp. 1261–1265
- [19] Bangi U.K.H., Han W., Yoo B., *ET AL.*: ‘Effects of successive additions of two capping ligands on the structural properties of PbO nanoparticles’, *J. Nanopart. Res.*, 2013, **15**, pp. 2070–2077
- [20] Morris T., Zubkov T.: ‘Steric effects of carboxylic capping ligands on the growth of the CdSe quantum dots’, *Colloids Surf. A Physicochem. Eng. Aspects*, 2014, **443**, pp. 439–449
- [21] Gallagher P.K., Schrey F.: ‘Thermal decomposition of some substituted barium titanyl oxalates and its effect on the semiconducting properties of the doped materials’, *J. Am. Ceram. Soc.*, 1963, **46**, pp. 567–573
- [22] Crosby L., Enterkin J., Rabuffetti F., *ET AL.*: ‘Wulff shape of strontium titanate nanocuboids’, *Surf. Sci.*, 2015, **632**, pp. L22–L25